

## Tight-binding Calculation of the Tunneling Spectra of the 122 type iron-based Superconductors in Normal State

S S JENA<sup>1</sup>, S K AGARWALLA<sup>1</sup> and G C ROUT<sup>2\*</sup>

<sup>1</sup>Dept of Applied physics and Ballistics, F.M. University, Odisha, 756019, India,

<sup>2</sup>Physics Enclave, Plot No. - 664/4825, Bhubaneswar- 751031, India,

\*Corresponding author: Email Id: gcr@iopb.res.in,

<sup>1</sup>Email Id: sushree@iopb.res.in.

*Received: 10. 6.2017 ; Revised : 28.6.2017 ; Accepted :16.7 2017*

**Abstract.** In order to describe the experimentally observed tunneling spectra of the 122 type iron-based superconducting systems, we have proposed here a tight-binding model calculation based upon one band model. We have considered electron hoppings upto second nearest neighbors as well as Heisenberg type spin-spin interaction upto second nearest neighbors. The magnetic interaction is considered within Hartree-Fock mean-field approximation and the temperature dependent spin density wave (SDW) gap is calculated by Zuvarev's Green's function technique. Finally the electron density of states (DOS) is computed numerically and its evolution is investigated by varying electron hoppings and the SDW couplings.

**Keywords:** Spin density wave (SDW), Scanning Tunneling Microscopy (STM)

**PACS:** 75.30.Fv, 68.37.Ef

### 1. Introduction

Recent discovery of iron-based superconductors has generated tremendous interests in searching for other high-transition-temperature superconductors and the underlying mechanism [1, 2]. The 11 family of FeAs based superconductors is RFeAsO<sub>1-x</sub>F<sub>x</sub> with R = La, Sm, Ce, Nd, Pr [3]. The 122 family of FeAs based superconductors, A<sub>1-x</sub>K<sub>x</sub>Fe<sub>2</sub>As<sub>2</sub> ( $x \approx 0.4$ ) with A = Ba, Ca, Sr with T<sub>C</sub> = 38 K has been discovered more recently [4]. Two common aspects of both 1111 and 122 families have been experimentally revealed.

Their parent compounds likely display an antiferromagnetic (AF) ordering of iron spins at low temperatures and are accompanied by lattice distortion. The 1111 system like CeFeAsO exhibits spin density wave (SDW) transition (T<sub>N</sub> =

140 K) and structural phase transition (SPT) (tetragonal to orthorhombic upon cooling) i.e,  $T_S = 155$  K [5]. The 122 systems like  $MFe_2As_2$  with  $M = Ba, Sr, Ca$  exhibit similar SDW and SPT transitions i.e,  $T_S/T_N = 142$  K ( $M = Ba$ ) [6],  $T_S/T_N = 171$  K ( $M = Ca$ ) [7] and  $T_S/T_N = 205$  K ( $M = Sr$ ) [8].

The iron-based superconductors exhibit the interplay between the orbital ordering and the superconductivity of the system with  $s^\pm$  pairing symmetry [9]. The  $FeSe_{1-x}$  11 structure with exhibit superconducting transition temperature  $T_C = 8$  K and JT distortion temperature  $T_S = 90$  K with no magnetic transition. The 122 structured  $Ba_{1-x}K_xFe_2As_2$  shows the tetragonal to orthorhombic transition at  $T_S = T_{SDW} = 81$  K with superconductivity occurring at  $T_C = 24$  K [10]. For 11 type  $Fe_{1.125}Te$ , the electron density of states (DOS) is obtained for a nonmagnetic system. The electronic states near the Fermi level are mostly of 3d character from the  $Fe_1$  atom with a smaller contribution from the excess  $Fe_2$  atom reflecting the low concentration of this site. The result is that the Fermi level lies exactly at a sharp peak of the  $Fe_2$  3d DOS indicating the magnetic instability [11]. The scanning tunneling microscopy (STM) study of 122 system,  $BaFe_{1.8}Co_{0.2}As_2$  exhibits the superconducting gap of magnitude  $\Delta = 6.25$  meV in absence of magnetic field [12].

Jena. et. al. have reported the role of SDW [13], Jahn Teller (JT) distortion [14] and interplay of JT effect and superconductivity in Fe-based superconductors within one band model approach [15]. Recently Jena. et. al. have reported the tight-binding study of lattice distortion and the tunneling spectra within two band model approach [16, 17]. More Recently Jena. et. al. have reported the theoretical study of the interplay of the structural distortion and the superconductivity (SC) with  $s^\pm$  pairing symmetry and the anisotropic tunneling conductance spectra [18, 19]. Based upon our earlier tight-binding model calculation on spin density wave (SDW) in iron-based superconductor [13], we present here the theoretical study of the evolution of the electron DOS of the 122-type iron-based systems and interpretation of the experimentally observed tunneling spectra. Here we present the model Hamiltonian in section 2, calculation of SDW gap and electron DOS in section 3. results and discussion in section 4 and the conclusion in section 5.

## **2. Hamiltonian Model**

Based upon our earlier case [13] for the iron-based  $M_xFe_{2-x}Se_2$  system, we propose a t-J type minimum one band model including tight-binding term and the spin interactions which can be written as

$$H = \sum \varepsilon_k C_{k\sigma}^+ C_{k\sigma} + H_M \quad (1)$$

where  $\epsilon_k$  is the single band dispersion within tight-binding approximation in the Fe<sub>2</sub>-Se<sub>2</sub> square lattice. It is written as  $\epsilon_k = -2t_1(\cos kx + \cos ky) - 4t_2 \cos kx \cdot \cos ky - \mu$  where  $t_1$  and  $t_2$  are respectively the nearest and the next-nearest-neighbor hopping integrals of electrons in the square lattice and  $kx$  and  $ky$  are the components of the electron momentum  $\vec{k}$  and  $\mu$  is the chemical potential. The Heisenberg spin-spin interaction among the 3d electrons of Fe ions is written as

$$H_M = J_1 \sum_{\langle ij \rangle} \vec{S}_i \cdot \vec{S}_j + J_2 \sum_{\langle\langle ij \rangle\rangle} \vec{S}_i \cdot \vec{S}_j \quad (2)$$

The first term in equation (3) represents the spin-spin interaction among the nearest-neighbor sites with coupling  $J_1$  and second term represents the next-nearest-neighbor sites with magnetic coupling  $J_2$ . The magnetic Hamiltonian given in equation (3) is written in terms of cartesian components of the spins in Fe<sub>2</sub>Se<sub>2</sub> – plane of the system. The components are converted to spin rising ( $S_j^+$ ) and spin lowering ( $S_j^-$ ) operators using the relation,  $S_j^+ = S_j^x + iS_j^y$ ,  $S_j^- = S_j^x - iS_j^y$ . Then the Hamiltonian is considered within Hartree-Fock mean-field approximation. The Fourier transformed Hamiltonian appears as,

$$H_M = \sum_{k,\sigma} \Delta_S(k) \langle C_{k\sigma}^+ C_{k+Q,-\sigma} \rangle \quad (3)$$

where the spin density wave (SDW) gap  $\Delta_S(k)$  in the Fe<sub>2</sub>-Se<sub>2</sub> plane is written as

$$\Delta_S(k) = \sum_{k,\sigma} J(k) \langle C_{k\sigma}^+ C_{k+Q,-\sigma} \rangle \quad (4)$$

The effective spin coupling is given by

$$J(k) = J_1(\cos kx + \cos ky) + 2J_2 \cos kx \cdot \cos ky \quad (5)$$

The SDW order arises due to Fermi surface nesting with a nesting wave vector  $Q = (\pi, \pi/2)$ . Under this condition the one band dispersion satisfies the condition  $\epsilon_{k+Q} = -\epsilon_k$ . The spin gap can be calculated from the Hamiltonian (1) and (5) using the relation for  $\Delta_S(k)$  given in equation (4).

### 3. Calculation of Green's functions and SDW Gap

The total Hamiltonian described in section 2 is solved by Zuvarev's Green's function technique [20] and finally the Green's functions involved in the calculation are given by,

$$G_1(k, \omega) = \langle\langle C_{k\sigma}; C_{k\sigma}^+ \rangle\rangle_\omega = \frac{1}{2\pi} \frac{\omega - \epsilon_{k+Q}}{D_0(\omega)} \quad (6)$$

$$G_2(k, \omega) = \langle\langle C_{k+Q, -\sigma}; C_{k\sigma}^+ \rangle\rangle_\omega = \frac{1}{2\pi} \frac{\Delta_S(k+Q)}{D_0(\omega)} \quad (7)$$

where  $D_0(\omega)$  appearing in the denominator of the equations (6) and (7) is written as,

$$D_0(\omega) = (\omega + \mu)^2 - (\omega + \mu)(\varepsilon_k + \varepsilon_{k+Q}) + \varepsilon_k \varepsilon_{k+Q} - \Delta_S(k) \Delta_S(k+Q) \quad (8)$$

Equating  $D_0(\omega)$  to zero, we find the quasi-particle dispersion bands which are given by,

$$\omega_{1k, 2k} = -2\mu + \left[ \frac{(\varepsilon_k + \varepsilon_{k+Q}) \pm \sqrt{(\varepsilon_k - \varepsilon_{k+Q})^2 + 4\Delta_S(k)\Delta_S(k+Q)}}{2} \right] \quad (9)$$

From the correlation function calculated from the Green's function in equation (9), the spin density wave gap is calculated using the relation given in equation (6) and is written as

$$\Delta_S(k) = \sum_{k, \sigma} J(k) \Delta_S(k+Q) \left[ \frac{f(\beta\omega_{1k}) - f(\beta\omega_{2k})}{\omega_{1k} - \omega_{2k}} \right] \quad (10)$$

where the Fermi distribution function is  $f(x) = [\exp(x) + 1]^{-1}$ . The electron density of states is directly proportional to the tunneling conductance spectra observed by the photoelectron spectroscopy. The electron density of states is calculated from the imaginary part of the electron Green's function and the expression is written as,

$$DOS = -2\pi \sum_{k, \sigma} \text{Im} [G_1(k, \omega + i\eta)] \quad (11)$$

where  $\eta$  is the small spectral width. The summation of electron wave vector  $k$  is converted into integral form for x- and y- components of the electron vector  $k$  for the whole Brillouin zone taking  $100 \times 100$  grid points. So we have  $\sum_{k, \sigma} \rightarrow \frac{2S}{(2\pi)^2} \int \int dk_x dk_y$  where 'S' is the area of the square lattice and the factor '2' arises due to the two spin orientations of the spin. The physical parameters appearing in the calculation are scaled by the nearest-neighbor hopping integral  $t_1 = 1$ .

The dimensionless parameters are the second-nearest-neighbor hopping integral  $t_2 = t_2/t_1 = -2.25$ , the nearest-neighbor spin coupling  $g_1 = J_1/t_1$ , next-nearest-neighbor spin coupling  $g_2 = J_2/t_1$ , SDW gap  $z = \Delta_S(0)/t_1$ , band energy  $c = \omega/t_1$  and temperature  $t = k_B T/t_1$ .

#### 4. Results and Discussion

As defined in equation (11) the electron density of states (DOS) of 122 type iron-based superconductors in normal state is computed for different values of the model parameters of the system. The different plots of DOS are shown in figures 1 to 3. Figure-1 shows the band energy dependent DOS in absence of any other interaction of the system. The DOS shows a energy dependent symmetric peak near the Fermi level at energy  $c = 0$  with a very narrow V-shaped gap for the nearest-neighbor (NN) electron hopping  $t_1=1$  of the system. When we take into account of second NN electron hopping with energy  $t_2 = -2.25$  in addition to the NN electron hopping  $t_1 = 1$ , we observe that the electron DOS is suppressed compared to the value observed for the NN electron hopping alone. It is obvious now that the NN electron hopping overestimates the DOS of the system. The second NN contribution is substantial and it can not be neglected. Again we have observed that the symmetric peak now shifts to the valence band lying below the Fermi level ( $c \approx 0$ ) indicating the larger weight of the electron DOS in the valence band compared to the value in the conduction band lying above the Fermi level. Further we have observed a wider V-shaped gap near the Fermi level indicating the nature of the electron dispersion of the iron-based systems. Hence it is obvious now that the electron DOS is asymmetric with respect to the Fermi level. It is to mention further that the electron DOS is very small at the Fermi level indicating that the system is not good conductor or a bad insulator [21].

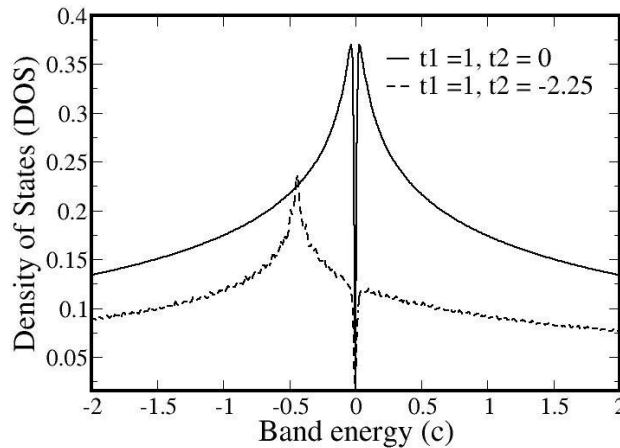


**Figure 1.** shows the plot of density of states (DOS) vs. band energy (c) for (continuous line)  $t_1 = 1, t_2 = 0$  and for (dotted lines)  $t_1 = 1, t_2 = -2.25$ .

There have been several reports of the occurrence of SDW order in the 122 type iron based superconductors [9]. We have self-consistently solved the temperature dependent SDW gap equation given in equation (10) and using the value of the gap parameter at given temperature. From the plot, we have computed the band energy dependent electron DOS for different spin interaction coupling as shown in figure 2. The inset of the figure 2 shows the temperature dependent SDW gap exhibiting mean-field behaviour with a sharp magnetic transition at Neel temperature  $t_N \approx 0.8$  ( $T_N \approx 160$  K) for the nearest-neighbor (NN) SDW coupling,  $g_1 = 2.6$  in absence of second nearest-neighbor (NN) SDW coupling,  $g_2 = 0$ . The SDW parameter  $g_1$  is so adjusted that we find the magnetic transition temperature  $t_N \approx 0.8$  ( $T_N \approx 150$  K) comparable to different values observed experimentally for example,  $T_N \approx 135$  K for the system  $Ba(Fe_{1-x}Co_x)_2As_2$ ,  $T_N \approx 205$  K for the system  $SrFe_2As_2$  [22,8].

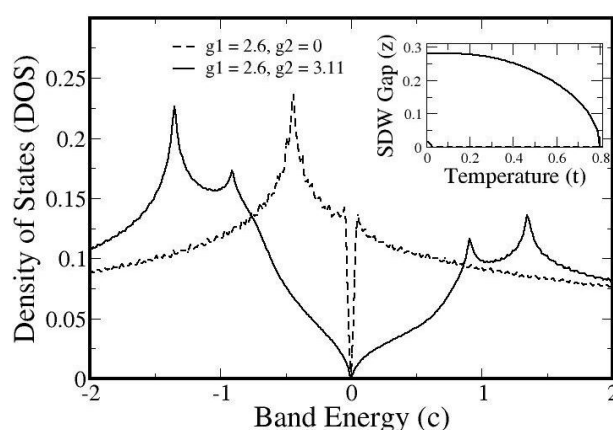


**Figure 2.** shows the plot of density of states (DOS) vs. band energy (c) for the variation of nearest nearest-neighbor spin couplings  $g_1 = 2.6$ ,  $g_2 = 0$  and for  $g_1 = 2.6$ ,  $g_2 = 3.11$  for fixed values of  $t_1 = 1$ ,  $t_2 = -2.25$ .

When we introduce the second NN SDW coupling  $g_2 = 3.11$  besides the NN SDW coupling  $g_1 = 2.6$ , we observed that the temperature dependent SDW gap is suppressed with corresponding suppression of the Neel temperature. This indicates that contribution of the second NN SDW coupling is substantial and it cannot be neglected. Taking the value of SDW coupling  $z_1 = 0.013$  for  $g_1 = 2.6$  and  $g_2 = 0$  and  $z_1 = 0.28$  for  $g_1 = 2.6$  and  $g_2 = 3.11$  at temperature  $t = 0.02$ , we have computed electron DOS as shown in figure 2. It is observed that the electron DOS exhibits a large V-shaped gap near Fermi level ( $c = 0$ ) separating the electron DOS of the conduction band lying above at energy  $c > 0$  and the DOS of

the valence band lying at energy  $c < 0$ . The weight-age of the electron density is much higher in valence band as compared to that of the conduction band. Further it is to mention that, we observe two splitted peaks on both the bands separated by the SDW gap energy. In presence of nearest and next-nearest-neighbor (NNN) SDW coupling the DOS is suppressed as compared to the DOS for nearest-neighbor (NN) SDW coupling  $g_1$ . The gap in the DOS near the Fermi level is widening due to the contribution of the second NN.

However, the gap between the two splitted peaks become larger due to the second NN SDW coupling indicating that the SDW gap is suppressed due to NNN SDW coupling as compared to NN SDW coupling alone. Thus, the NNN electron hopping has some contribution which cannot be neglected. There-fore, we have considered here NN and NNN SDW coupling for the SDW interaction in the iron-based superconductors.

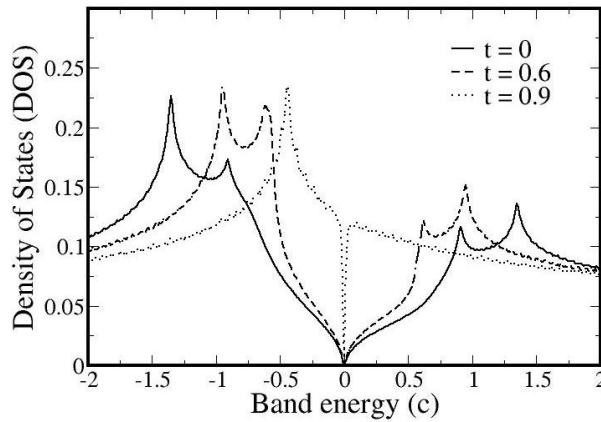


**Figure 3.** shows the plot of density of states (DOS) vs. band energy ( $c$ ) for different temperatures  $t = 0, 0.6, 0.9$  for fixed values  $t_1 = 1, t_2 = -2.25$  and  $g_1 = 2.6, g_2 = 3.11$ .

Figure 3 shows the band energy dependent electron DOS for the iron-based superconductors for different temperatures  $t = 0, 0.6, 0.9$ . At temperature  $t = 0.9$ , above the Neel temperature in the paramagnetic phase, we observe a sharp peak below the Fermi level ( $c = 0$ ) lying in the valence band besides a narrow V-shaped gap at Fermi level. At temperature  $t = 0.6$ , below the Neel temperature in the SDW interaction region, we observe a wider SDW gap at  $c = 0$  separating the electron DOS of the conduction and valence bands. The peaks split into two in both the bands separated by the energy of the magnitude of the SDW gap. At temperature  $t = 0$ , the gap at  $c = 0$ , widens further and the splitted peaks either

side of the Fermi level are further separated by the SDW gap of higher magnitude. This indicates that the SDW gap increases with decrease of temperature becoming the maximum at  $t = 0$ .

## 5. Conclusions

We have proposed a tight-binding model for the 122 type iron-based superconductors in normal state taking nearest neighbor (NN) and next-nearest neighbor (NNN) electron hoppings as well as spin density wave (SDW) interactions. The SDW interaction is treated here within mean-field approximation. The electron densities are computed for different values of electron hoppings and SDW couplings. It is observed that second NN electron hopping and SDW interactions are substantial and they give realistic values of the magnitude of SDW gap besides the realistic electron DOS.

## References

- [1] Y Kamhira et.al., *J. Am. Chem. Soc.* **130** 3296 (2008).
- [2] H. Takahashi et.al., *Nature London* **453** 376 (2008).
- [3] X. H. Chen et.al., *Nature London* **453** 761 (2008).
- [4] M. Rotter et.al., *Phys. Rev. Lett.* **101** 107006 (2008).
- [5] J. Zhao et.al., *Nature Matter.* **7** 953 (2008).
- [6] Q. Y. Huang et.al., *Phys. Rev. Lett.*, **101** 257003 (2008).
- [7] F. T. Ronning et. al., *J. Phys. Condens. Matter* **20** 322201(2008).
- [8] C. N. Krellner et.al., *Phys. Rev. B* **78** 100504 (R) (2008).
- [9] G. R. Stewart, *Rev.Mod. Phys. Vol.* **83** 1589 (2011).
- [10] A. E. Bohmer et al. *arxiv:* 1412.7038v2 (2014).
- [11] Fengjie Ma et. al., *Phys. Rev. Lett.* **102** 177003 (2009).
- [12] Yi Yin et. al., *Phys. Rev. Lett.* **102** 097002 (2009).
- [13] S. S. Jena and G. C Rout, *Adv. Sc. Letts*, Vol. **22**, No. 2, pp. 327-330(4) (2016).
- [14] S. S. Jena, S. K. Panda and G. C. Rout, *AIP Conf. Proceedings* **1728** 020082 (2016).
- [15] S. S. Jena, S. K. Agarwalla and G. C. Rout, *AIP Conf. Proceedings* (In Press) (2015).
- [16] S. S. Jena, S. K. Agarwalla and G. C. Rout, *Orissa Journal Physics* Vol. **23**, No. 2 pp. 169-177 (2016).
- [17] S. S. Jena, S. K. Agarwalla and G. C. Rout, *Orissa Journal Physics* Vol. **24**, No. 1 pp. 39-44 (2017).
- [18] S. S. Jena, S. K. Agarwalla and G. C. Rout., *AIP Conf. Proc.* **1832**, 130025 (2017).
- [19] S. S. Jena, S. K. Agarwalla and G. C. Rout., *Int. J. Nano and Biomaterials*, (2017) (Communicated).
- [20] D. N. Zubarev, *sov. Phys. Usp.* **3** 320 (1960).
- [21] K. Haule et. al., *Phys. Rev. Lett.* **100** 226402 (2008).
- [22] S. Nandi et.al., *Phys. Rev. Lett.* **104** 057006 (2010).